bile/BC structures. There might be aberrant fucose overloading of the sorting machinery in HepG2 cells because the numbers of BC structures of HepG2 cells are limited. We also reported that AFP had several kinds of alpha1−6 fucosylated structures, although the percentages were small.[4] Comparison of oligosaccharide structures on AFP derived from the BC structures with the conditioned medium is our greatest interest, although the analysis is impossible because of low levels of AFP in the BC structures.

Characters of human hepatoblastoma, HepG2 cells, correspond to neither HCCs nor normal hepatocytes. It has been reported that a number of cell lines, such as Huh7 cells and WIF-B9 cells, can form BC structures.[29] However, we were unable to obtain a sufficient amount of protein from the BC structures of cells other than HepG2. The numbers of BC structures in the other cell lines examined were much lower than those in HepG2 under our culture conditions. Therefore, our data in the present study might be limited in HepG2 cells. It is well accepted that the secretory pathway is dramatically changed in many cases in cancers and especially in HCC. To know whether or not increases of fucosylated AFP (AFP-L3) in sera of patients with HCC are dependent on the abnormality of the secretory pathway of fucosylated glycoproteins, a study using much more human liver tissues bearing HCC should be performed. Another possibility is that an abnormality of fucose-specific lectin in the liver, if it exits, is induced in HCC tissues.

Early detection of HCC is essential for successful treatment. The recent development of highly sensitive detection systems for AFP-L3 enables us to detect HCC at an early stage.[26,30] On the other hand, increased fucosylation in sera of HCC patients are not limited to AFP. There are many reports that increases in the levels of fucosylation of serum glycoproteins occur with the development of HCC.[31−33] Clarification of the mechanism underlying the polarized secretion of fucosylated glycoproteins in the liver will lead to the development of novel glyco-cancer biomarkers.

AUTHOR INFORMATION

Corresponding Author

*Tel: +81-6-6879-2590. Fax: +81-6-6879-2590. E-mail: emiyoshi@sahs.med.osaka-u.ac.jp.

Notes

The authors declare no competing financial interest.

ACKNOWLEDGMENTS

This work was supported by the New Energy and Industrial Technology Development Organization (NEDO) as a part of the Developing Technology Project for Implementing Sugar Chain Functions in Japan. This work was also supported in part by the Global COE Program of Osaka University funded by the Ministry of Education, Culture, Sports, Science, and Technology of Japan and a Grant-in-Aid for Scientific Research (A), No. 21249038, from the Japan Society for the Promotion of Science.

ABBREVIATIONS

AFP-L3, L3 fraction of alpha-fetoprotein; HCC, hepatocellular carcinoma; Fut8, alpha1−6 fucosyltransferase; FX, human homologue of GDP-4-keto-6-deoxymannose-3,5-epimerase-4-reductase; BC, bile canaliculus; GMD, GDP-mannose-4,6-dehydratase; AOL, *Aspergillus oryzae* lectin; FBS, fetal bovine serum; DKD, double knock-down; shRNA, small hairpin RNA; SDS-PAGE, sodium dodecylsulfate-polyacrylamide gel electrophoresis; TBS, Tris-buffered saline; TBST, TBS containing 0.05% Tween 20; LCA, *Lens culinaris*; PA, pyridylamino; HPLC, high-performance liquid chromatography; LC-ESI-MS/MS, liquid chromatography-electrospray ionization-tandem mass spectrometry; AGP, alpha1-acid glycoprotein

REFERENCES

(1) Morinaga, T.; Sakai, M.; Wegmann, T. G.; Tamaoki, T. Primary structures of human alpha-fetoprotein and its mRNA. *Proc. Natl. Acad. Sci. U. S. A.* **1983**, *80* (15), 4604−8.

(2) Yoshima, H.; Mizuochi, T.; Ishii, M.; Kobata, A. Structure of the asparagine-linked sugar chains of alpha-fetoprotein purified from human ascites fluid. *Cancer Res.* **1980**, *40* (11), 4276−81.

(3) Yamashita, K.; Taketa, K.; Nishi, S.; Fukushima, K.; Ohkura, T. Sugar chains of human cord serum alpha-fetoprotein: characteristics of *N*-linked sugar chains of glycoproteins produced in human liver and hepatocellular carcinomas. *Cancer Res.* **1993**, *53* (13), 2970−5.

(4) Nakagawa, T.; Miyoshi, E.; Yakushijin, T.; Hiramatsu, N.; Igura, T.; Hayashi, N.; Taniguchi, N.; Kondo, A. Glycomic analysis of alpha-fetoprotein L3 in hepatoma cell lines and hepatocellular carcinoma patients. *J. Proteome Res.* **2008**, *7* (6), 2222−33.

(5) Taketa, K. Alpha-fetoprotein: reevaluation in hepatology. *Hepatology* **1990**, *12* (6), 1420−32.

(6) Uozumi, N.; Yanagidani, S.; Miyoshi, E.; Ihara, Y.; Sakuma, T.; Gao, C. X.; Teshima, T.; Fujii, S.; Shiba, T.; Taniguchi, N. Purification and cDNA cloning of porcine brain GDP-L-Fuc:*N*-acetyl-beta-D-glucosaminide alpha1−6fucosyltransferase. *J. Biol. Chem.* **1996**, *271* (44), 27810−7.

(7) Yanagidani, S.; Uozumi, N.; Ihara, Y.; Miyoshi, E.; Yamaguchi, N.; Taniguchi, N. Purification and cDNA cloning of GDP-L-Fuc:*N*-acetyl-beta-D-glucosaminide:alpha1−6 fucosyltransferase (alpha1−6 FucT) from human gastric cancer MKN45 cells. *J. Biochem.* **1997**, *121* (3), 626−32.

(8) Noda, K.; Miyoshi, E.; Uozumi, N.; Yanagidani, S.; Ikeda, Y.; Gao, C.; Suzuki, K.; Yoshihara, H.; Yoshikawa, K.; Kawano, K.; Hayashi, N.; Hori, M.; Taniguchi, N. Gene expression of alpha1−6 fucosyltransferase in human hepatoma tissues: a possible implication for increased fucosylation of alpha-fetoprotein. *Hepatology* **1998**, *28* (4), 944−52.

(9) Noda, K.; Miyoshi, E.; Nakahara, S.; Ihara, H.; Gao, C. X.; Honke, K.; Yanagidani, S.; Sasaki, Y.; Kasahara, A.; Hori, M.; Hayashi, N.; Taniguchi, N. An enzymatic method of analysis for GDP-L-fucose in biological samples, involving high-performance liquid chromatography. *Anal. Biochem.* **2002**, *310* (1), 100−6.

(10) Noda, K.; Miyoshi, E.; Gu, J.; Gao, C. X.; Nakahara, S.; Kitada, T.; Honke, K.; Suzuki, K.; Yoshihara, H.; Yoshikawa, K.; Kawano, K.; Tonetti, M.; Kasahara, A.; Hori, M.; Hayashi, N.; Taniguchi, N. Relationship between elevated FX expression and increased production of GDP-L-fucose, a common donor substrate for fucosylation in human hepatocellular carcinoma and hepatoma cell lines. *Cancer Res.* **2003**, *63* (19), 6282−9.

(11) Tonetti, M.; Sturla, L.; Bisso, A.; Benatti, U.; De Flora, A. Synthesis of GDP-L-fucose by the human FX protein. *J. Biol. Chem.* **1996**, *271* (44), 27274−9.

(12) Kristiansen, T. Z.; Bunkenborg, J.; Gronborg, M.; Molina, H.; Thuluvath, P. J.; Argani, P.; Goggins, M. G.; Maitra, A.; Pandey, A. A proteomic analysis of human bile. *Mol. Cell. Proteomics* **2004**, *3* (7), 715−28.

(13) Nakagawa, T.; Uozumi, N.; Nakano, M.; Mizuno-Horikawa, Y.; Okuyama, N.; Taguchi, T.; Gu, J.; Kondo, A.; Taniguchi, N.; Miyoshi, E. Fucosylation of *N*-glycans regulates the secretion of hepatic glycoproteins into bile ducts. *J. Biol. Chem.* **2006**, *281* (40), 29797−806.

(14) Nakagawa, T.; Takeishi, S.; Kameyama, A.; Yagi, H.; Yoshioka, T.; Moriwaki, K.; Masuda, T.; Matsumoto, H.; Kato, K.; Narimatsu, H.; Taniguchi, N.; Miyoshi, E. Glycomic analyses of glycoproteins in

bile and serum during rat hepatocarcinogenesis. *J. Proteome Res.* **2010**, *9* (10), 4888–96.
(15) Sormunen, R.; Eskelinen, S.; Lehto, V. P. Bile canaliculus formation in cultured HEPG2 cells. *Lab. Invest.* **1993**, *68* (6), 652–62.
(16) van, I. S. C.; Hoekstra, D. Polarized sphingolipid transport from the subapical compartment changes during cell polarity development. *Mol. Biol. Cell* **2000**, *11* (3), 1093–101.
(17) Zegers, M. M.; Hoekstra, D. Mechanisms and functional features of polarized membrane traffic in epithelial and hepatic cells. *Biochem. J.* **1998**, *336* (Pt 2), 257–69.
(18) Bastaki, M.; Braiterman, L. T.; Johns, D. C.; Chen, Y. H.; Hubbard, A. L. Absence of direct delivery for single transmembrane apical proteins or their "Secretory" forms in polarized hepatic cells. *Mol. Biol. Cell* **2002**, *13* (1), 225–37.
(19) Miyoshi, E.; Ihara, Y.; Hayashi, N.; Fusamoto, H.; Kamada, T.; Taniguchi, N. Transfection of *N*-acetylglucosaminyltransferase III gene suppresses expression of hepatitis B virus in a human hepatoma cell line, HB611. *J. Biol. Chem.* **1995**, *270* (47), 28311–5.
(20) Tomiya, N.; Awaya, J.; Kurono, M.; Endo, S.; Arata, Y.; Takahashi, N. Analyses of *N*-linked oligosaccharides using a two-dimensional mapping technique. *Anal. Biochem.* **1988**, *171* (1), 73–90.
(21) Takahashi, N.; Kato, K. GALAXY (glycoanalysis by the three axes of MS and chromatography): a web application that assists structural analyses of *N*-glycans. *Trends Glycosci. Glycotechnol.* **2003**, *15* (84), 235–51.
(22) Misonou, Y.; Shida, K.; Korekane, H.; Seki, Y.; Noura, S.; Ohue, M.; Miyamoto, Y. Comprehensive clinico-glycomic study of 16 colorectal cancer specimens: elucidation of aberrant glycosylation and its mechanistic causes in colorectal cancer cells. *J. Proteome Res.* **2009**, *8* (6), 2990–3005.
(23) Tateno, H.; Nakamura-Tsuruta, S.; Hirabayashi, J. Comparative analysis of core-fucose-binding lectins from *Lens culinaris* and *Pisum sativum* using frontal affinity chromatography. *Glycobiology* **2009**, *19* (5), 527–36.
(24) Becker, D. J.; Lowe, J. B. Fucose: biosynthesis and biological function in mammals. *Glycobiology* **2003**, *13* (7), 41R–53R.
(25) Kuno, A.; Ikehara, Y.; Tanaka, Y.; Angata, T.; Unno, S.; Sogabe, M.; Ozaki, H.; Ito, K.; Hirabayashi, J.; Mizokami, M.; Narimatsu, H. Multilectin assay for detecting fibrosis-specific glyco-alteration by means of lectin microarray. *Clin. Chem.* **2011**, *57* (1), 48–56.
(26) Hanaoka, T.; Sato, S.; Tobita, H.; Miyake, T.; Ishihara, S.; Akagi, S.; Amano, Y.; Kinoshita, Y. Clinical significance of the highly sensitive fucosylated fraction of alpha-fetoprotein in patients with chronic liver disease. *J. Gastroenterol. Hepatol.* **2011**, *26* (4), 739–44.
(27) Kitagawa, Y.; Sano, Y.; Ueda, M.; Higashio, K.; Narita, H.; Okano, M.; Matsumoto, S.; Sasaki, R. *N*-Glycosylation of erythropoietin is critical for apical secretion by Madin-Darby canine kidney cells. *Exp. Cell Res.* **1994**, *213* (2), 449–57.
(28) Comunale, M. A.; Rodemich-Betesh, L.; Hafner, J.; Wang, M.; Norton, P.; Di Bisceglie, A. M.; Block, T.; Mehta, A. Linkage specific fucosylation of alpha-1-antitrypsin in liver cirrhosis and cancer patients: implications for a biomarker of hepatocellular carcinoma. *PLoS One* **2010**, *5* (8), e12419.
(29) Decaens, C.; Durand, M.; Grosse, B.; Cassio, D. Which in vitro models could be best used to study hepatocyte polarity? *Biol. Cell* **2008**, *100* (7), 387–98.
(30) Tamura, Y.; Igarashi, M.; Kawai, H.; Suda, T.; Satomura, S.; Aoyagi, Y. Clinical advantage of highly sensitive on-chip immunoassay for fucosylated fraction of alpha-fetoprotein in patients with hepatocellular carcinoma. *Dig. Dis. Sci.* **2010**, *55* (12), 3576–83.
(31) Block, T. M.; Comunale, M. A.; Lowman, M.; Steel, L. F.; Romano, P. R.; Fimmel, C.; Tennant, B. C.; London, W. T.; Evans, A. A.; Blumberg, B. S.; Dwek, R. A.; Mattu, T. S.; Mehta, A. S. Use of targeted glycoproteomics to identify serum glycoproteins that correlate with liver cancer in woodchucks and humans. *Proc. Natl. Acad. Sci. U. S. A.* **2005**, *102* (3), 779–84.
(32) Comunale, M. A.; Lowman, M.; Long, R. E.; Krakover, J.; Philip, R.; Seeholzer, S.; Evans, A. A.; Hann, H. W.; Block, T. M.; Mehta, A. S. Proteomic analysis of serum associated fucosylated glycoproteins in the development of primary hepatocellular carcinoma. *J. Proteome Res.* **2006**, *5* (2), 308–15.
(33) Comunale, M. A.; Wang, M.; Hafner, J.; Krakover, J.; Rodemich, L.; Kopenhaver, B.; Long, R. E.; Junaidi, O.; Bisceglie, A. M.; Block, T. M.; Mehta, A. S. Identification and development of fucosylated glycoproteins as biomarkers of primary hepatocellular carcinoma. *J. Proteome Res.* **2009**, *8* (2), 595–602.

DOI 10.1002/pmic.201100655 *Proteomics* 2012, *12*, 2190–2202

RESEARCH ARTICLE

Proteomic analysis of gingival crevicular fluid for discovery of novel periodontal disease markers

Sachio Tsuchida[1], Mamoru Satoh[1,2,3], Hiroshi Umemura[1,2], Kazuyuki Sogawa[1,2], Yusuke Kawashima[4], Sayaka Kado[3], Setsu Sawai[1,2], Motoi Nishimura[1,2], Yoshio Kodera[2,4], Kazuyuki Matsushita[1,2] and Fumio Nomura[1,2]

[1] Department of Molecular Diagnosis, Graduate School of Medicine, Chiba University, Chiba, Japan
[2] Clinical Proteomics Research Center, Chiba University Hospital, Chiba, Japan
[3] Chemical Analysis Center, Chiba University, Chiba, Japan
[4] Laboratory of Biomolecular Dynamics, Department of Physics, School of Science, Kitasato University, Minato, Tokyo, Japan

The protein composition of gingival crevicular fluid (GCF) may reflect the pathophysiology of periodontal diseases. A standard GCF proteomic pattern of healthy individuals would serve as a reference to identify biomarkers of periodontal diseases by proteome analyses. However, protein profiles of GCF obtained from apparently healthy individuals have not been well explored. As a step toward detection of proteomic biomarkers for periodontal diseases, we applied both gel-based and gel-free methods to analyze GCF obtained from healthy subjects as compared with supragingival saliva. To ensure optimized protein extraction from GCF, a novel protocol was developed. The proteins in GCF were extracted with high yield by urea buffer combined with ultrafiltration and the intensity of spots with supragingival saliva and GCF was compared using agarose two-dimensional electrophoresis. Eight protein spots were found to be significantly more intense in GCF. They included superoxide dismutase 1 (SOD1), apolipoprotein A-I (ApoA-I), and dermcidin (DCD). Moreover, GCF proteins from healthy subjects were broken down into small peptide fragments and then analyzed directly by LC-MS/MS analysis. A total of 327 proteins including ApoA-I, SOD1, and DCD were identified in GCF. These results may serve as reference for future proteomic studies searching for GCF biomarkers of periodontal diseases.

Received: December 19, 2011
Revised: March 30, 2012
Accepted: April 12, 2012

Keywords:
Biomedicine / Gingival crevicular fluid / Periodontal disease

1 Introduction

Periodontal disease is characterized by destruction of hard tissue and soft connective tissue constituents of the periodontium [1]. Better physiological understanding of periodontal disease would improve the diagnosis, treatment, and prevention of periodontitis [2]. Recent studies suggested that C-reactive protein (CRP) and other systemic markers of inflammation were elevated in periodontal diseases and effective periodontal therapy may decrease CRP values [3–6]. Periodontal disease is an inflammatory lesion initiated by gram-negative periodontal bacterial pathogens such as *Porphyromonas gingivalis* [7]. Therefore, gingival keratinocytes in periodontium are the primary line of defense against bacterial infection.

The components of gingival crevicular fluid (GCF) may include breakdown products of host epithelial and connective tissues, products of host cell in the periodontium, and products derived from the subgingival microbial plaque [8–10]. These factors could be possible candidates for predictors of disease activity. A variety of proteins detected in GCF play a central part in periodontal tissue turnover. Consequently,

Correspondence: Dr. Fumio Nomura, Department of Molecular Diagnosis (F8), Graduate School of Medicine, Chiba University, 1-8-1 Inohana, Chuo-ku, Chiba 260-8670, Japan
E-mail: fnomura@faculty.chiba-u.jp
Fax: +81-43-226-2169

Abbreviations: ApoA-I, apolipoprotein A-I; **AU**, arbitrary units; **CRP**, C-reactive protein; **DCD**, dermcidin; **GCF**, gingival crevicular fluid; **MMP**, matrix metalloproteinase; **SOD1**, superoxide dismutase 1; **WB**, Western blotting

analysis of a biochemical marker in GCF may help in diagnosis as it also predicts the progression of periodontal disease [11]. Therefore, investigations to detect diagnostic markers of periodontal diseases are warranted.

Recently, many studies have applied expression proteomics to identify proteins whose abundance levels were altered by disease. Proteomic analysis is a novel method for detecting biomarkers in tumors and inflammatory diseases. Approaches based on a combination of 2DE and MS analysis for the identification of proteins in a variety of inflammatory diseases and cancer were demonstrated. The technique of proteomic analysis using 2DE and MS has the ability to monitor changes that occur in the protein complement of tissues and subcellular compartments. We have shown that the agarose 2DE method had advantages over the conventional 2DE in that they have a higher loading capacity than 2DE with IPG gel for IEF [12]. This agarose 2DE not only allows for large-scale quantitative comparison of protein but also is able to resolve high molecular mass protein larger than 150 kDa [13].

Compared to other biofluids, such as serum/plasma, urine, and cerebrospinal fluid, the protein profiles of GCF have not yet been explored. The previous report by Bostanci et al. was based on the gel-free method alone [14]. Since diagnostic values of biomarker candidates discovered by proteome analyses are always evaluated in comparison with normal subjects, a standard GCF proteomic pattern from healthy individuals would serve as a reference.

As a step toward future biomarker discovery, we conducted both gel-based and gel-free proteomic analysis of GCF obtained from apparently healthy subjects as compared with supragingival saliva.

2 Materials and methods

2.1 Extraction of GCF

GCF samples were collected from 16 volunteers (ten males, six females, the mean age of 36.0 years). Prior to sample collection, the subjects rinsed their mouths. All volunteers provided informed consent to participate in the procedures. All were in good general health with no history of antimicrobial or antiinflammatory therapy or periodontal treatment for 6 months before the start of the study. Since smoking is a risk factor for periodontal disease, the current study did not include smokers. Clinical parameters such as probing depth, clinical attachment level, gingival bleeding index, full-mouth plaque scores, and bleeding scores of each group were recorded. The probing depth at six sites for each tooth was measured using the PCP-UNC15 probe (Hu-Friedy, Chicago, IL, USA). For recording the loss of clinical attachment level, the cemento-enamel junction was used as a reference. Participants were first examined for periodontal disease. Full-mouth Löe–Silness gingival index and clinical attachment loss were measured at six sites (mesio-, mid-, disto-buccal/palatal, or lingual) per tooth using the PCP-UNC15 probe with a diameter of 0.5 mm at the tip [15, 16]. The periodontal disease subjects were assigned to three groups (moderate, mild, and severe) on the basis of overall clinical diagnostic criteria and the classification of periodontal diseases by the American Academy of Periodontology (AAP) 1999 [17] (Table 1). The study sample included in this study was as follows: healthy; $n = 50$, mild periodontal disease; $n = 30$, moderate periodontal disease; $n = 30$, severe periodontal disease; $n = 50$.

GCF was collected from the labial side of maxillary incisors without crown and restoration. Supra-gingival plaque was carefully removed from the tooth by a curette, the teeth were rinsed with saline, and the sampling sites were isolated with cotton rolls and dried. Each sample site was carefully isolated using cotton rolls to avoid saliva contamination. Absorbent paper points (ZIPPERER®, Munich, Germany) were gently inserted into the gingival crevice and left in place for 30 s. Mechanical irritation was avoided and the absorbent paper points contaminated with blood were discarded. Theses paper points were stored at −80°C for further processing.

2.2 Sample preparation

A mixture of 7 M urea and 2 M thiourea including 2% CAPS and 2 mM DTT was added to GCF in paper points. The paper points were vortexed for 10 min and centrifuged at 20 000 × g for 15 min. After centrifugation, paper points were ultrafiltered using Ultrafree-MC (Millipore, Bedford, MA). The protein concentration of the extract was estimated by the method of Bradford, with bovine serum albumin as a standard.

2.3 2DE

GCF samples from five healthy subjects were applied to agarose IEF gel, and first-dimensional IEF was conducted at 12 000 Vh at 4°C. This was followed by fixation in 10% TCA and 5% sulfosalicylic acid for 45 min at room temperature. After washing in deionized water for 45 min, the agarose gel was transferred to 10–20% gradient of polyacrylamide gel and 2DE was performed. The protein spots on the 2DE gels were stained with silver (2-D silver stain II "DAIICHI," Daiichi Pure Chemicals Co., Ltd., Osaka, Japan).

2.4 SDS-PAGE and Western blot analysis

A total of 10 μg/μL GCF protein was separated by SDS-PAGE on a 10–20% polyacrylamide gradient gel and transferred to PVDF membranes (Millipore, Bedford, MA) in a Bio-Rad Trans-Blot apparatus (Bio-Rad, Hercules, CA). The membranes were blocked at room temperature in PBS with pH 7.5, containing 5% skim milk and 0.05% Tween 20. Anti-Dermicidin mouse monoclonal antibody (G-81: Santa

Table 1. Clinical parameters

Group	PPD (mm)	CAL (mm)	GI	FMPS (%)	FMBS (%)
Healthy ($n = 5$)	1.2 ± 0.2	1.3 ± 0.3	0	38.6 ± 23.5	8.6 ± 20.5
Mild periodontal disease ($n = 3$)	2.7 ± 0.2*	2.9 ± 0.4*	0.7 ± 0.2*	48.8 ± 25.7	46.7 ± 22.5*
Moderate periodontal disease ($n = 3$)	4.7 ± 0.3*	4.6 ± 0.2*	1.3 ± 0.2*	51.7 ± 35.6	61.8 ± 33.7*
Severe periodontal disease ($n = 5$)	7.5 ± 0.3*	7.8 ± 0.3*	1.5 ± 0.3*	60.8 ± 33.5	70.9 ± 23.4*

PPD, probing depth; CAL, clinical attachment level; GI, gingival index; FMPS, full-mouth plaque scores; FMB, full-mouth bleeding scores. The asterisk indicates significant difference from the healthy group (Mann–Whitney *U*-test, $p < 0.05$).

Cruz Biotechnology Inc., Santa Cruz, CA) diluted 1:1000, anti-Apolipoprotein A-I mouse monoclonal antibody (5F4: Cell Signaling Technology, MA) diluted 1:1000, and anti-Superperoxidase 1 rabbit polyclonal antibody in blocking buffer were used as primary antibodies diluted 1:1000 with the same buffer, and the membranes were incubated in it overnight at 4°C. Subsequently, the membranes were washed three times in phosphate-buffered saline (PBS) containing 0.05% Tween 20 and incubated for 1 h with goat anti-mouse IgG HRP (Bio-Rad Laboratories, Hercules, CA) diluted 1:2000, and goat anti-rabbit IgG HRP (Bio-Rad Laboratories, Hercules, CA) diluted 1:2000 in blocking buffer used as secondary antibodies. The bands were visualized by use of ECL (GE Healthcare UK Ltd., Buckinghamshire, UK) Band intensities were quantified using TotalLab TL12 imaging analysis software (Shimadzu Co., Ltd. Kyoto, Japan) and were represented by arbitrary units (AU).

2.5 In-gel digestion of proteins

The gel was cut into small pieces, destained in 50% ACN/50 mM NH_4HCO_3, and washed with deionized water. The gel pieces were dehydrated in 100% ACN for 15 min, and then dried in a SpeedVac Evaporator (Wakenyaku, Kyoto, Japan) for 45 min. The gel pieces were rehydrated in 10–30 μL of 25 mM Tris-HCl/20% CAN containing 25 ng/μL trypsin (Trypsin sequence grade, Roche) for 45 min. After removal of the unabsorbed solution, the gel pieces were incubated in 10–20 μL of 50 mM Tris-HCl/20% ACN for 20 h at 37°C. The solution containing digested fragments of proteins was transferred to a new tube, and the peptide fragments remaining in the gel were extracted in 5% formic acid/50% ACN for 20 min at room temperature.

2.6 In-solution digestion of proteins

A mixture of 4 M urea and 100 mM ammonium bicarbonate were added to the paper point containing GCF. The paper point was vortexed for 10 min and centrifuged at 20 000 × g for 15 min. Then, 2 μL of 200 mM DTT added and incubated at 57°C for 30 min. After incubation, 2 μL of 600 mM iodacetoamide was added and incubated at room temperature for 30 min in dark. Five microliters of trypsin with 26 μL of distilled water was incubated at 37°C for 6 h. The resulting peptides were added to 5 μL of 5% TFA or 5% formic acid.

2.7 Protein identification

In-gel digested peptides were injected into a trap column: 0.3 × 5 mm L-trap column (Chemicals Evaluation and Research Institute, Saitama, Japan), and an analytical column: 0.1 × 50 mm Monolith column (AMR, Tokyo, Japan), which was attached to a HPLC system (Nanospace SI-2; Shiseido Fine Chemicals, Tokyo, Japan). The flow rate of the mobile phase was 1 μL/min. The solvent composition of the mobile phase was programed to change in 35-min cycles with varying mixing ratios of solvent A (2% v/v CH_3CN and 0.1% v/v HCOOH) to solvent B (90% v/v CH_3CN and 0.1% v/v HCOOH): 5–50% B 20 min, 50–95% B 1 min, 95% B 3 min, 95–5% B 1 min, 5% B 10 min. Purified peptides were introduced from HPLC to an LTQ-XL (Thermo Scientific, CA, USA), an ion trap mass spectrometer (ITMS), via an attached Pico Tip (New Objective, MA, USA). The MS and MS/MS peptide spectra were measured in a data-dependent manner according to the manufacturer's operating specifications. The Mascot search engine (Matrix science, London, UK) was used to identify proteins from the mass and tandem mass spectra of peptides. Peptide mass data were matched by searching the Human International Protein Index database (IPI, July 2008, 72 079 entries, European Bioinformatics Institute) using the MASCOT engine. The minimum criterion of the probability-based MASCOT/MOWSE score was set with 5% as the significant threshold level.

In-solution digested peptides were injected into a trap column (C_{18}, 0.3 × 5 mm, DIONEX, CA, USA), and an analytical column (C_{18}, 0.075 × 120 mm, Nikkyo Technos, Tokyo, Japan), which was attached to the Ultimate 3000 (DIONEX, CA, USA). The flow rate of the mobile phase was 300 nL/min. The solvent composition of the mobile phase was programed to change in 120-min cycles with varying mixing ratios of solvent A (2% v/v CH_3CN and 0.1% v/v HCOOH) to solvent B (90% v/v CH_3CN and 0.1% v/v HCOOH): 5–10% B 5 min, 10–13.5% B 35 min, 13.5–35% B 65 min, 35–90% B 4 min, 90% B 0.5 min, 90–5% B 0.5 min, 5% B 10 min. Purified peptides were introduced from HPLC to LTQ-Orbitrap XL (Thermo Scientific, San Jose, CA, USA), a hybrid ion-trap

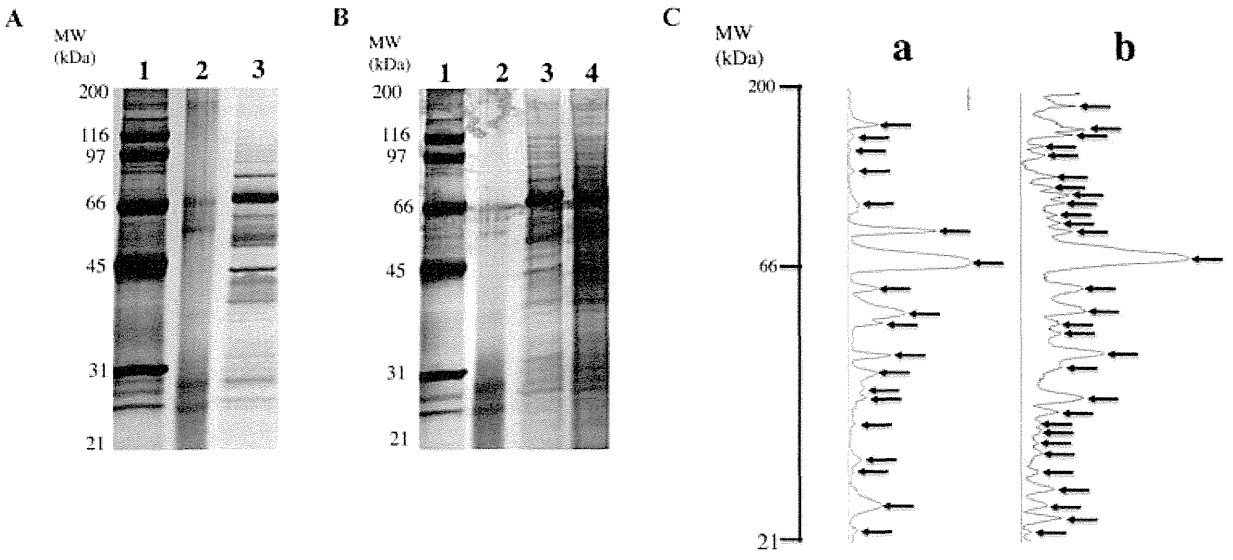

Figure 1. SDS-PAGE gel of GCF proteins extracted by PBS buffer and urea buffer combined with ultrafiltration and stained with Silver. (A) Five microgram of protein was loaded/lane. Lane 1, molecular weight (MW) standard; Lane 2, peptide standard; Lane 3, PBS buffer extractions. Lane 1, MW standard; Lane 2, peptide standard; Lane 3, urea buffer extractions and Lane 4, urea buffer combined with ultrafiltration extractions (B). (C) Densitometric analysis of the gel shown in panels A and B. One peak (arrows) corresponds to one protein band. Lane 3 in panel A corresponds to A. Lane 4 in panel B corresponds to B.

Fourier transform mass spectrometer. The MASCOT search engine (version 2.2.6, Matrixscience, London, UK) was used to identify proteins from the mass and tandem mass spectra of peptides. Peptide mass data were matched by searching the UniProtKB database (SwissProt 2010x, November 2010, 9590 entries). Database search parameters were: peptide mass tolerance, 1.2 Da; fragment tolerance, 0.6 Da; enzyme was set to trypsin, allowing up to one missed cleavage; variable modifications, methionine oxidation. The minimum criteria of protein identification were set as false discovery rate (FDR) $< 1\%$. The FDR was estimated by searching against a randomized decoy database created by the Mascot Perl program supplied by Matrix Science (London, UK).

2.8 Statistical analysis

The differences in values between periodontal and healthy subjects were analyzed by Mann–Whitney *U*-test and Kruskal–Wallis test with the Dwass–Steel–Chritchlow–Flinger method. Differences at $p < 0.05$ were considered statistically significant.

3 Results

3.1 Comparison of two different protein extraction methods

To develop an optimized protein extraction method, either PBS buffer or urea buffer combined with ultrafiltration was employed as an extraction protocol in the first step of this study. We evaluated the extraction ability of the two methods used to extract proteins from GCF by SDS-PAGE, as shown in Fig. 1A and B. Nineteen protein bands (A: marked by arrowheads) were observed in the PBS buffer method and 30 protein bands (B: marked by arrowheads) in the urea buffer combined with ultrafiltration (Fig. 1C). Greater amounts of extracted proteins were obtained using urea buffer combined with ultrafiltration. Proteins in the GCF were extracted with high yield by urea buffer treatment followed by ultrafiltration using an ultrafiltration device.

3.2 Identification of altered expressed protein in GCF

To search for novel GCF markers useful for the diagnosis of periodontal disease, we compared the protein spots of GCF with supragingival saliva using agarose 2DE analysis. Hundred micrograms total protein of GCF and supragingival saliva were separated by agarose 2DE, and proteins were visualized by Silver-staining (Fig. 2A and B). These spots were detected and quantitated with imaging analysis software, and then statistical analysis was performed across the 10 gels. We carefully compared the 2D image with Silver-staining gel and picked altered protein spots manually. When comparing the intensity of spots between supragingival saliva and GCF, eight protein spots were found to be significantly more intense in GCF. In contrast, no protein spots were more intense in supragingival saliva. The proteins in which the expression levels were different are shown in respective gels (Fig. 2A and B).

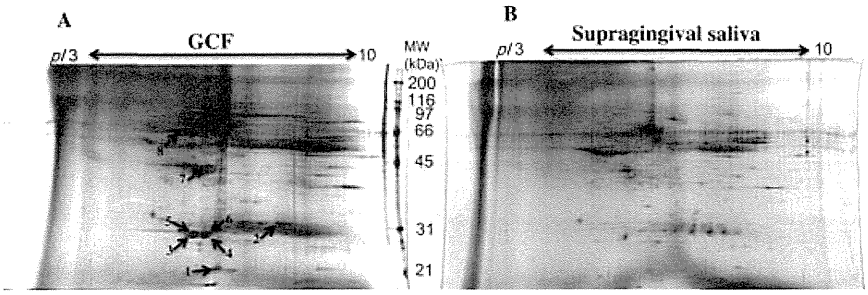

Figure 2. Proteome analysis of GCF and supragingival saliva using agarose 2DE. Conventional agarose 2DE patterns were visualized by Silver-staining. Eight increased protein spots in GCF are displayed with arrows. Eight protein spots cut from this gel were identified by LC-MS/MS and are shown in arrows (increased protein spots).

The increased eight proteins spots in the GCF were cut out from the conventional agarose 2DE gel and were subjected to in gel digestion, followed by LC-MS/MS analysis. They included Haptoglobin, Superoxide dismutase 1(SOD1), ALB protein, Apolipoprotein A-I (ApoA-I), and Dermcidin (DCD) (Table 2).

3.3 Liquid digestion and LC-MS/MS analysis

Whole proteins were enzymatically digested into small peptide fragments with uniform characteristics and then analyzed directly by LC-MS/MS analysis, so-called shotgun proteomics. Shotgun proteomics have been widely used for detection of disease markers, for diseases such as cancer and systemic inflammation. GCF samples from five healthy subjects were pooled and subjected to trypsin digestion, followed by identification by LC-MS/MS. Three hundred twenty-seven proteins including ApoA-I, SOD1, and DCD were identified in GCF by LC-MS/MS analysis. Other identified proteins include cathelicidin, cathepsin G, cystatin-C, interleukin-1 receptor antagonist protein, Lysozyme C, macrophage migration inhibitory factor, matrix metalloproteinase-8, -9 (MMP-8,-9), metalloproteinase inhibitor 1(TIMP-1), neutrophil defensin 1, and vitamin D-binding protein, whose

Table 2. LC-MS/MS identification of increased protein spots on 2DE gels that are differently expressed in GCF

Spot number[a)]	Protein name	MW[b)]	p*I*[c]	Score[d]	Sequence coverage[e)]	MS/MS[f)] (unique)	Fold increase[g)]
1	HP Haptoglobin precorsor	46 693	6.28	118	7%	4	1.58
	SOD1 Superoxide dismutase	15 926	5.7	61	9%	1	
2	ALB ALB protein	45 130	5.77	75	3%	1	1.51
	IGL@ IGL@ protein	24 777	5.93	52	8%	1	
3	APOA1 Apolipoprotein A-I precursor	30 759	5.56	557	50%	12	1.77
	APOA1 Apolipoprotein A-I precursor	30 759	5.56	713	41%	11	
4	IGK@ IGK@ protein	25 757	5.94	204	28%	4	1.77
	DCD Dermcidin precursor	11 277	6.08	74	10%	1	
5	APOA1 Apolipoprotein A-I precursor	30 759	5.56	571	41%	11	1.73
6	APOA1 Apolipoprotein A-I precursor	30 759	5.56	392	43%	11	1.75
	IGKV1-5 IGKV1-5 protein	26 218	6.3	136	15%	2	
7	SERPINA1 Isoform 1 of Alpha-1-antitrypsin precursor	46 707	5.37	241	18%	7	1.62
	IGHV3OR16-13	53 054	6.46	136	8%	3	
8	ALB Uncharacterized protein ALB	71 658	6.33	151	9%	6	1.61

a) Protein spots were described in Fig 2.
b) Theoretical molecular mass (Da) based on NCBI BLAST database.
c) Theoretical p*I* based on Swiss-Prot database.
d) SEQUEST score of candidate proteins.
e) Sequence coverage of MS/MS analysis of protein.
f) MS/MS unique peptide.
g) Intensity of spots in 2D-PAGE gel of 10 matched samples (GCF versus supragingival saliva) was measured.

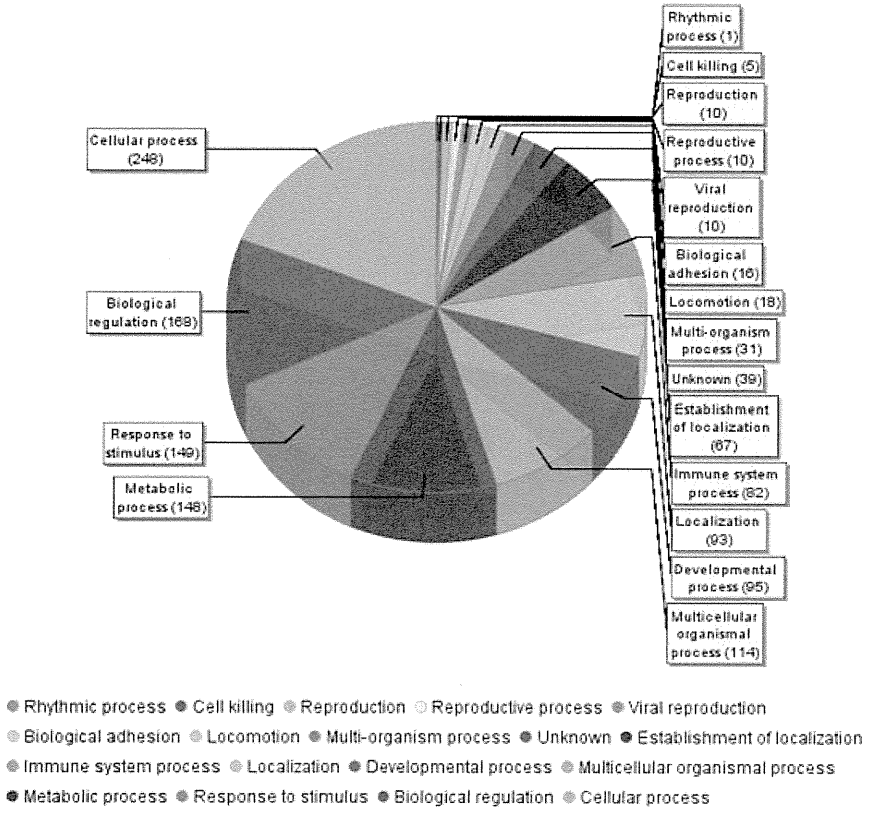

Figure 3. Functional annotation of GCF from healthy subjects using Gene Ontology Annotation Database. Identified proteins have immune system, metabolic function, response to stimulus, and biological regulation.

expression have been previously reported to be related to periodontal disease [18–26].

On the other hand, they included Annexin A5, Annexin A6, Interleukin-36 gamma (IL-36γ), lamin A/C, periplakin, moesin, which are associated with tumors and systemic diseases in human (Supporting Information Table S1).

Figure 3 shows the functional annotation of GCF from healthy subjects using Gene Ontology Annotation Database. Identified proteins in GCF have biological regulation (168 proteins), response to stimulus (149 proteins), metabolic process (148 proteins), and immune system (82 proteins). Figure 4 shows the distribution of proportion of GCF proteins according to their source of origin in healthy subjects. Proteins from bacteria, firmicutes, yeast, and virus are present in the GCF (Table 3). MS/MS Unique peptide of Elongation factor 1-alpha 1 from *Saccharomyces cerervisiae* matched the MS/MS unique peptide from human alone. Moreover, proteins from periodontal pathogenic bacteria such as *P. gingivalis* or *Actinobacillus actinomycetemcomitans* were not detected.

Further investigations are necessary to evaluate whether these proteins in GCF may have a role in diagnosis of various periodontal diseases.

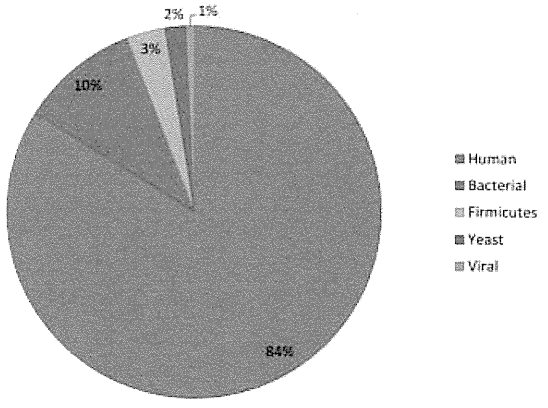

Figure 4. Distribution of the proportion of GCF proteins according to their source of origin in healthy subjects. The proportions are expressed as percentage (%) of the total protein in healthy subjects. Five sources of origin were identified: human, bacterial, firmicutes, yeast, viral.

Table 3. LC-MS/MS identification of GCF proteins derived from nonhuman organisms

Organism	Identified proteins	Accession number[a)]	Molecular weight[b)]	MS/MS unique peptide[c)]	MS/MS unique peptide (HUMAN)[d)]
Bacterial					
Acidovorax ebreus	Methionyl-tRNA synthetase	SYM_ACIET (+1)	77 kDa	1	0
Acinetobacter sp.	Malonyl-CoA O-methyltransferase BioC	BIOC_ACIAD	Unknown	1	0
Acinetobacter sp.	Urease subunit gamma	URE3_ACIAD (+6)	11 kDa	1	0
Agrobacterium rhizogenes	Putative replication protein C	REPC_AGRRH	44 kDa	1	0
Anaeromyxobacter dehalogenans	Methionyl-tRNA formyltransferase	FMT_ANAD2 (+2)	33 kDa	1	0
Blochmannia pennsylvanicus	Glucose-6-phosphate isomeras	G6PI_BLOPB	63 kDa	1	0
Bordetella avium	Serine hydroxymethyltransferase	GLYA_BORA1 (+1)	45 kDa	1	0
Bordetella pertussis	Cyclolysin secretion/processing ATP-binding protein CyaB	CYAB_BORPE	78 kDa	1	0
Bradyrhizobium japonicum	Protein slyX homolog	SLYX_BRAJA	8 kDa	1	0
Bradyrhizobium japonicum	Cytochrome c-type biogenesis protein CycH	CYCH_BRAJA	40 kDa	1	0
Buchnera aphidicola subsp. Acyrthosiphon pisum	Isoleucyl-tRNA synthetase	SYI_BUCA5 (+3)	110 kDa	1	0
Buchnera aphidicola subsp. Baizongia pistaciae	DNA-directed RNA polymerase subunit beta	RPOC_BUCBP	157 kDa	1	0
Buchnera aphidicola subsp. Cinara cedri	50S ribosomal protein L2	RL2_BUCCC	31 kDa	1	0
Coxiella burnetii	Elongation factor Tu	EFTU_COXBN (+15)	44 kDa	1	0
Delftia acidovorans	Probable ubiquinone biosynthesis protein UbiB	UBIB_DELAS	60 kDa	1	0
Desulfobacterium autotrophicum	Threonyl-tRNA synthetase	SYT_DESAH	72 kDa	1	0
Desulfococcus oleovorans	Alanine racemase	ALR_DESOH	41 kDa	1	0
Dichelobacter nodosus	Chaperone protein DnaK	DNAK_DICNV (+2)	70 kDa	1	0
Enterobacter aerogenes	Glyceraldehyde-3-phosphate dehydrogenase	G3P_ENTAE	31 kDa	1	0
Erwinia tasmaniensis	Triosephosphate isomerase	TPIS_ERWT9	27 kDa	1	0
Escherichia coli	Transcriptional activator perA	PERA_ECO27	32 kDa	1	0
Geobacter bemidjiensis	Threonyl-tRNA synthetase	SYT_GEOBB (+3)	72 kDa	1	0
Geobacter sp.	Dihydroorotase	PYRC_GEOSF (+1)	45 kDa	1	0
Helicobacter pylori	Uncharacterized protein jhp_0176	Y190_HELPJ	58 kDa	1	0
Lawsonia intracellularis	Ribonuclease Y	RNY_LAWIP	Unknown	1	0
Magnetococcus sp.	Protein translocase subunit SecF	SECF_MAGSM	Unknown	1	0
Magnetococcus sp.	DNA replication and repair protein recF	RECF_MAGSM	42 kDa	1	0
Methylobacterium nodulans	Chaperone protein DnaK	DNAK_METNO	69 kDa	1	0

Table 3. Continued

Organism	Identified proteins	Accession number[a)]	Molecular weight[b)]	MS/MS unique peptide[c)]	MS/MS unique peptide (HUMAN)[d)]
Methylocella silvestris	ATP synthase subunit delta	ATPD_METSB	20 kDa	1	0
Novosphingobium aromaticivorans	N-Succinylglutamate 5-semialdehyde dehydrogenase	ASTD_NOVAD	51 kDa	1	0
Pseudomonas mendocina	Adenosylhomocysteinase	SAHH_PSEMY	51 kDa	1	0
Psychromonas ingrahamii	Phospho-N-acetylmuramoyl-pentapeptide-transferase	MRAY_PSYIN	40 kDa	1	0
Rhodobacter sphaeroides	Phosphoglycerate kinase	PGK_RHOS5	41 kDa	1	0
Rickettsia bellii	Aconitate hydratase	ACON_RICBR (+2)	98 kDa	1	0
Salmonella agona	Flagellar P-ring protein	FLGI_SALA4 (+13)	38 kDa	1	0
Serratia proteamaculans	Alanyl-tRNA synthetase	SYA_SERP5	96 kDa	1	0
Shewanella oneidensis	Chemotaxis response regulator protein-glutamate methylesterase of group 1 operon	CHEB1_SHEON	39 kDa	1	0
Vibrio vulnificus	3-Octaprenyl-4-hydroxybenzoate carboxy-lyase	UBID_VIBVY	69 kDa	1	0
Wolbachia pipientis	Chromosomal replication initiator protein dnaA	DNAA_WOLPM	53 kDa	1	0
Xylella fastidiosa	Glycyl-tRNA synthetase beta subunit	SYGB_XYLF2 (+3)	80 kDa	1	0
Firmicutes					
Bacillus anthracis	Enolase	ENO_BACAA (+15)	46 kDa	1	0
Bacillus subtilis	Probable glucarate dehydratase	GUDH_BACSU	51 kDa	1	0
Clostridium kluyveri	DNA ligase	DNLJ_CLOK1 (+11)	75 kDa	1	0
Clostridium tetani	Probable 2-phosphosulfolactate phosphatase	COMB_CLOTE	26 kDa	1	0
Enterococcus faecalis	ATP-dependent helicase/ deoxyribonuclease subunit B	ADDB_ENTFA	139 kDa	1	0
Lactobacillus acidophilus	UPF0348 protein LBA1527	Y1527_LACAC	44 kDa	1	0
Listeria innocua	Phosphoribosylamine–glycine ligase	PUR2_LISIN	46 kDa	1	0
Oceanobacillus iheyensis	Chaperone protein DnaK	DNAK_OCEIH	67 kDa	1	0
Staphylococcus aureus	Conserved virulence factor B	CVFB_STAA3 (+8)	34 kDa	1	0
Streptococcus pyogenes serotype M1	Elongation factor Tu	EFTU_STRP1 (+12)	44 kDa	1	0
Streptococcus suis	Ribosomal RNA small subunit methyltransferase H	RSMH_STRS2 (+4)	36 kDa	1	0

Table 3. Continued

Organism	Identified proteins	Accession number[a)]	Molecular weight[b)]	MS/MS unique peptide[c)]	MS/MS unique peptide (HUMAN)[d)]
Symbiobacterium thermophilum	Chorismate synthase	AROC_SYMTH	42 kDa	1	0
Thermoanaerobacter tengcongensis	Triosephosphate isomerase	TPIS_THETN	27 kDa	1	0
Yeast					
Geobacter sp.	Dihydroorotase	PYRC_GEOSF (+1)	45 kDa	1	0
Saccharomyces cerevisiae	Elongation factor 1-alpha 1	EF1A1_HUMAN (+3)	50 kDa	2	2
Saccharomyces cerevisiae	Phosphatidylglycerol phospholipase C	PGC1_YEAST	unknown	1	0
Saccharomyces cerevisiae	Malate dehydrogenase, mitochondrial	MDHM_YEAST	36 kDa	1	0
Saccharomyces cerevisiae	Ras-related protein SEC4	SEC4_YEAST	24 kDa	1	0
Saccharomyces cerevisiae	Histone H2B.1	H2B1_YEAST (+1)	14 kDa	1	0
Saccharomyces cerevisiae	Heat shock protein SSC1, mitochondrial	HSP77_YEAST	71 kDa	1	0
Virus					
Acanthamoeba polyphaga mimivirus	Uncharacterized protein R292	YR292_MIMIV	22 kDa	1	0
Carnation etched ring virus	Virion-associated protein	VAP_CERV	unknown	1	0
Infectious salmon anemia virus	Fusion glycoprotein F0	FUS_ISAVC	49 kDa	1	0

GCF proteins from healthy subjects ($n = 5$) were identified using LC-MS/MS. Identified proteins are listed.
a) Reference for protein identification.
b) Theoretical molecular mass based on Swiss–Prot database.
c) MS/MS unique peptide.
d) MS/MS unique peptide (human database).

3.4 Expression levels of ApoA-I, SOD1, and DCD in healthy subjects and patients with periodontal disease

Among the identified proteins, we looked at the proteins identified by the two methods (gel-based and gel-free) in common and also focused on disease-associated proteins, whose expression levels have not been well studied in periodontal disease. Three proteins, namely SOD1, DCD, ApoA-I met the above conditions.

ApoA-I is the major protein component of high-density lipoprotein (HDL) in plasma. ApoA-I has a specific role in lipid metabolism [27]. The superoxide dismutases (SOD) are the most important line of antioxidant enzyme defense system against reactive oxygen species (ROS). SOD1, one of the human SOD, is also known as superoxide dismutase [Cu-Zn] [28]. DCD was identified as a gene for an antimicrobial peptide DCD-1 in human sweat glands. This peptide has antimicrobial function and a range of biological functions [29].

Western blot analyses of ApoA-I, SOD1, and DCD were performed to compare the expression levels of these proteins in GCF obtained from healthy controls and those from subjects with periodontal disease. The GCF in severe periodontal disease group exhibited higher expression of SOD1 and DCD than the healthy control group ($p = 0.0131$, Fig. 5B, $p = 0.0162$, Fig. 5C). However, the expression level of ApoA-I did not differ between the two groups (Fig. 5A).

4 Discussion

As a fluid lying in close proximity to periodontal tissue, GCF is the principal target in biomarker search for periodontal diseases. However, it is not an easy task to collect GCF samples from periodontal pockets during the active phase of periodontitis without any bleeding. GCF samples are usually collected by periopaper strips. In this study, we collected GCF samples using absorbent paper points. Paper points are widely used for the collection of subgingival plaque or other oral samples to analyze the microbes especially the presence of periodontal pathogenic bacteria [30]. In addition, the very apical portions of the periodontal pocket are accessible, as the niche of front-line species. This procedure using paper points could minimize bleeding from periodontal pocket during GCF sample collection.

Conventionally, protein extraction from GCF in periodontal disease research has been performed with PBS buffer alone [14, 31]. However, we suspected that the capacity of PBS buffer alone was not enough to remove substantial amount of proteins from paper points used for GCF collection. Therefore, as the first step toward biomarker discovery for periodontal diseases, we developed a novel extraction protocol and found that use of urea buffer combined with ultrafiltration with Ultrafree-MC was satisfactory as indicated in Fig. 1. Ultrafiltration is the process of separating ex-

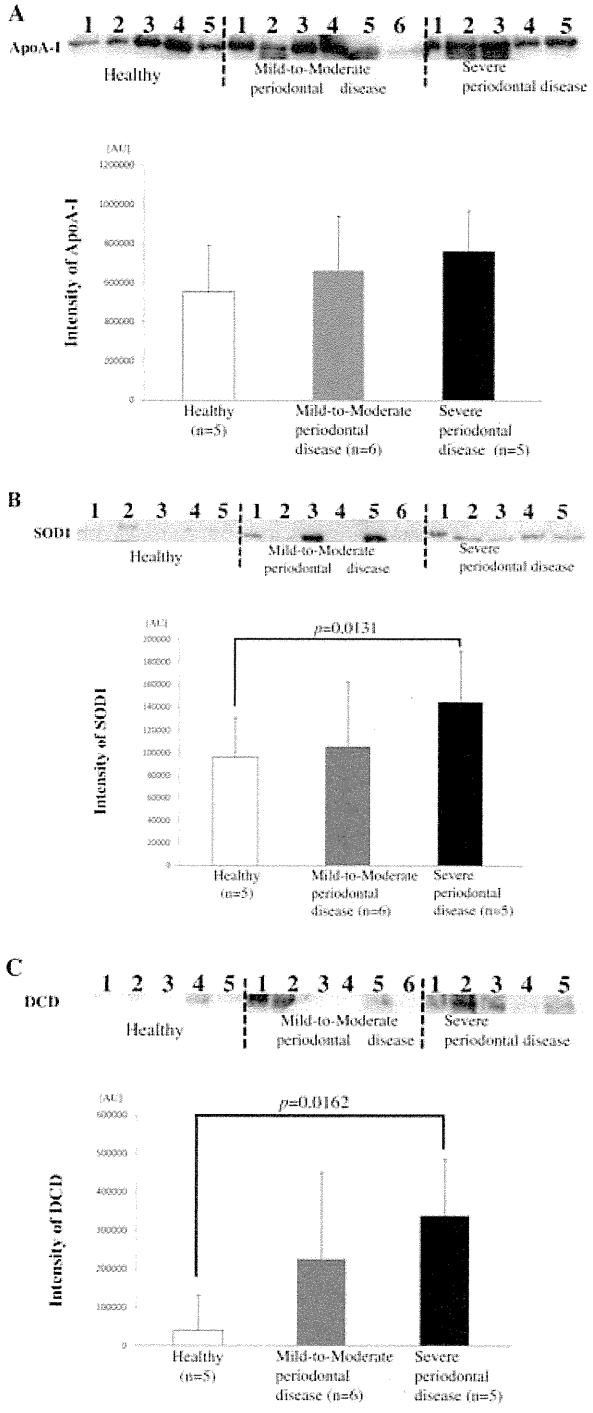

Figure 5. Western blot analysis of ApoA-I, SOD1, and DCD in GCF. Total protein prepared from samples from healthy subjects and mild-to-moderate and severe periodontal patients were separated by electrophoresis on 10% to 20% polyacrylamide gradient gel, and immunoblotted with anti-ApoA-I antibody (A), anti-SOD1 antibody (B), and anti-DCD antibody (C). The intensity of each band was measured using imaging analysis. Data are expressed as the mean ± SD. The SOD1 and DCD band volumes were significantly increased in the severe periodontal disease group when compared with those of the control group ($p < 0.05$).

tremely small particles and dissolving molecules from samples. Ultrafree-MC is available in a range of microporous membranes (http://www.millipore.com/ catalogue/module/c7554) for removing particulates from solutions and from ultrafiltration membranes for protein concentration as well as protein removal prior to HPLC. These methods could remove substantial amount of proteins from paper points and could serve as effective pretreatment of GCF when used as a source for discovery of diagnostic markers for periodontal diseases.

In this study, low-abundance proteins in GCF samples from healthy subjects were separated by agarose 2DE method. The agarose 2DE has a higher loading capacity than the conventional 2DE with IPG gel for IEF [12]. Therefore, the agarose 2DE method would be preferable when GCF is present in relatively small amounts in the body. GCF contains substances from the host as well as those from microorganisms in the subgingival and supragingival plaque. A standard GCF proteomic pattern of healthy individuals would serve as a reference to search for biomarkers of periodontal diseases by proteome analyses. However, protein profiles of GCF obtained from apparently healthy individuals have not been well explored. As a second step, we applied both gel-based and gel-free methods to analyze GCF obtained from healthy subjects as compared with supragingival saliva. With the gel-based method using the agarose 2D-DIGE, eight proteins preferentially expressed in GCF were identified; out of these eight proteins, SOD1, ApoA-I, and DCD were identified by the gel-free method as well. The SOD comprise the most important line of antioxidant enzyme defense system against ROS [32]. Excess production of ROS contributes to tissue damage in a large spectrum of diseases such as diabetes, rheumatoid arthritis, and cancer [33, 34]. ROS has also been implicated in the pathogenesis of periodontal disease. Kimura et al. have shown increased generation rate of ROS from peripheral blood polymorphonuclear leukocytes in chronic adult periodontal disease [35]. In addition, lipopolysaccharide (LPS) induces the production of ROS in organs such as liver and kidney. LPS, the glycolipid of the outer membrane of gram-negative bacteria, elicits inflammatory responses leading to the release of various proinflammatory cytokines and contributes to pathophysiology of periodontal diseases. As the third step, we compared the expression levels of SOD1, Apo-A1 and DCD in GCF in healthy subjects and patients with periodontal diseases. In this study, there was a significant difference in the SOD1 concentration between the two groups (Fig. 4B). This is in agreement with the increased SOD1 activity in GCF reported by Akalin et al. in periodontal disease [36]. However, the exact role of SOD1 in GCF for the pathogenesis of periodontal disease remains to be established in further studies. The SOD1 gene is conserved in *S. cerevisiae* whose proteins were detected in GCF samples in the proteome study performed [14]. Since the sequence coverage is low (9%) and just one MS/MS unique peptide was used to identify the protein spot number 1 (Fig. 2), there is a possibility that the increased amount of SOD1 protein in GCF samples of periodontal disease reflects the existence of *S. cerevisiae*. Therefore, we conducted database homology searches using Blast search. Results indicated that the amino-acid sequence similarity of SOD1 from *S. cerevisiae* and human was very weak (56%). Furthermore, we performed identification of GCF proteins using the yeast (*S. cerevisiae*) database. There was no protein equivalent to SOD1 from *S. cerevisiae*. Therefore, we can conclude that the amino acid sequence of SOD1 from *S. cerevisiae* was not included in the MS/MS unique peptide in this study. Indeed, we confirmed SOD1 expression in Human gingival fibroblast by Western blot analysis (data not shown). It is interesting to note that SOD1 was observed in the Human Gingival Fibroblast. In the future, we plan to explore the mechanism of SOD1 expression in GCF.

We identified an antimicrobial peptide DCD for the first time in GCF using agarose 2DE method. DCD levels were found to be significantly increased in GCF compared with supragingival saliva (Fig. 2). Furthermore, the results of Western blot test clearly showed that DCD levels were significantly greater in GCF obtained from patients with periodontal disease than that from healthy subjects. Periodontal disease is an inflammatory disease initiated by gram-negative bacteria, such as *P. gingivalis* [37]. *Porphyromonas gingivalis* is the bacteria most strongly associated with periodontal disease. DCD including antimicrobial peptides play multiple roles in immune defense. These peptides have been demonstrated to kill gram-negative and gram-positive bacteria, mycobacteria, enveloped viruses, fungi, etc [38]. DCD could defend against inflammatory microbial peptide at the gingival epithelial surface. A detailed analysis to determine the exact roles of DCD in periodontal disease may be required.

On the other hand, using the gel-free method, a total of 327 proteins were identified in GCF samples from healthy subjects (Supporting Information Table S1) [14]. Interestingly, tissue inhibitors of metalloproteinase (TIMP-1) were identified in GCF from healthy subjects, MMPs are able to degrade most proteins of the extracellular matrix. MMPs are counteracted by the TIMPs, which inhibit MMP activity and thereby restrict ECM breakdown. A disturbed balance of MMPs, such as MMP-8, MMP-9, and TIMPs is found in various pathologic conditions, including rheumatoid arthritis, cancer, and periodontal disease [18]. Moreover, there are a number of reports indicating the role of MMPs in health and disease, but information on TIMPs is limited, especially with respect to their role in oral disease including periodontal disease.

The distribution of the proportion of GCF proteins according to their source of origin in healthy subjects is shown in Fig. 4 and Table 3. As a result, proteins from expected periodontal pathogenic bacteria such as, *P. gingivalis* or *A. actinomycetemcomitans* were not detected. *P. gingivalis* and *A. actinomycetemcomitans* are strongly associated with periodontal disease status and disease progression. In this study, subgingival plaque must be collected together with GCF in healthy subjects as well. We suppose that subgingival microbiota from healthy subjects contains just a little percent of periodontal pathogenic bacteria, even if it is beyond the

detectable limit. The major purpose of this investigation was to reveal proteomic patterns of GCF obtained from apparently healthy subjects. Proteins derived from *P. gingivalis* and *A. actinomycetemcomitans* were not included in the results obtained. It is likely that proteins derived from these periodontopathic microbes may be detectable in GCF obtained from patients with periodontitis. In this context, it should be noted that subgingival microbiota composition is different between healthy subjects and subjects with periodontitis [39, 40].

A total of 327 proteins included Annexin A5, Annexin A6, IL-36γ, lamin A/C, periplakin, and moesin, which are reported to be involved in a variety of human diseases. In the present study, we focused on SOD1, apo-A1, and DCD proteins that were identified by the two methods in common. We plan to investigate the association of other proteins and peptides among the 327 candidates with periodontal diseases.

In summary, we first described a novel protocol for effective protein extraction from GCF and then conducted the gel-based and gel-free proteome analyses of GCF proteins in comparison with supragingival saliva. A total of 327 GCF proteins were identified. Also, it was found that SOD1 and DCD were significantly increased in GCF obtained from periodontal patients. It remains to be investigated how other GCF proteins identified in this study are related to periodontal diseases.

5 References

[1] Schroeder, H. E., Listgarten, M. A., The gingival tissues: the architecture of periodontal protection. *Periodontol 2000.* 1997, *13*, 91–120.

[2] Listgarten, M. A., Pathogenesis of periodontitis. *J. Clin. Periodontol.* 1986, *13*, 418–430.

[3] D'Aiuto, F., Nibali, L., Parkar, M., Suvan, J. et al., Short-term effects of intensive periodontal therapy on serum inflammatory markers and cholesterol. *J. Dent. Res.* 2005, *84*, 269–273.

[4] D'Aiuto, F., Parkar, M., Andreou, G., Suvan, J. et al., Periodontitis and systemic inflammation: control of the local infection is associated with a reduction in serum inflammatory markers. *J. Dent. Res.* 2004, *83*, 156–160.

[5] Adonogianaki, E., Mooney, J., Kinane, D. F., Detection of stable and active periodontitis sites by clinical assessment and gingival crevicular acute-phase protein levels. *J. Periodontal. Res.* 1996, *31*, 135–143.

[6] Sakallioğlu, E. E., Lütfioğlu, M., Sakallioğlu, U., Diraman, E. et al., Fluid dynamics of gingiva in diabetic and systemically healthy periodontitis patients. *Arch. Oral. Biol.* 2008, *53*, 646–651.

[7] Tezal, M., Scannapieco, F. A., Wactawski-Wende, J., Grossi, S. G. et al., Supragingival plaque may modify the effects of subgingival bacteria on attachment loss. *J. Periodontol.* 2006, *77*, 808–813.

[8] Curtis, M. A., Griffiths, G. S., Price, S. J., Coulthurst, S. K. et al., The total protein concentration of gingival crevicular fluid. Variation with sampling time and gingival inflammation. *J. Clin. Periodontol.* 1988, *15*, 628–632.

[9] Figueredo, C. M., Areas, A., Miranda, L. A., Fischer, R. G. et al., The short-term effectiveness of non-surgical treatment in reducing protease activity in gingival crevicular fluid from chronic periodontitis patients. *J. Clin. Periodontol.* 2004, *31*, 615–669.

[10] Golub, L. M., Kleinberg, I., Gingival crevicular fluid: a new diagnostic aid in managing the periodontal patient. *Oral. Sci. Rev.* 1976, *8*, 49–61.

[11] Lamster, I. B., Ahlo, J. K., Analysis of gingival crevicular fluid as applied to the diagnosis of oral and systemic diseases. *Ann. NY Acad. Sci.* 2007, *1098*, 216–229.

[12] Oh-Ishi, M., Maeda, T., Disease proteomics of high-molecular-mass proteins by two-dimensional gel electrophoresis with agarose gels in the first dimension (Agarose 2-DE). *J. Chromatogr. B. Analyt. Technol. Biomed. Life Sci.* 2007, *849*, 211–222.

[13] Seimiya, M., Tomonaga, T., Matsushita, K., Nomura, F. et al., Identification of novel immunohistochemical tumor markers for primary hepatocellular carcinoma; clathrin heavy chain and formiminotransferase cyclodeaminase. *Hepatology* 2008, *48*, 519–530.

[14] Bostanci, N., Heywood, W., Mills, K., Parkar, M. et al., Application of label-free absolute quantitative proteomics in human gingival crevicular fluid by LC/MS^E (gingival exudatome). *J. Proteome. Res.* 2010, *9*, 2191–2199.

[15] Löe, H., Silness, J., Periodontal disease in pregnancy. I. Prevalence and severity. *Acta. Odontol. Scand.* 1963, *21*, 533–551.

[16] Löe, H., The gingival index, the plaque index and the retention index systems. *J. Periodontol.* 1967, *38*, 610–616.

[17] Armitage, G. C., Development of a classification system for periodontal diseases and conditions. *Ann. Periodontol.* 1999, *4*, 1–6.

[18] Türkoğlu, O., Emingil, G., Kütükçüler, N., Atilla, G., Gingival crevicular fluid levels of cathelicidin LL-37 and interleukin-18 in patients with chronic periodontitis. *J. Periodontol.* 2009, *80*, 969–976.

[19] Goutoudi, P., Diza, E., Arvanitidou, M., Effect of periodontal therapy on crevicular fluid interleukin-1beta and interleukin-10 levels in chronic periodontitis. *J. Dent.* 2004, *32*, 511–520.

[20] Kunimatsu, K., Mine, N., Muraoka, Y., Kato, I. et al., Identification and possible function of cathepsin G in gingival crevicular fluid from chronic adult periodontitis patients and from experimental gingivitis subjects. *J. Periodontal Res.* 1995, *30*, 51–57.

[21] Lah, T. T., Babnik, J., Schiffmann, E., Turk, V. et al., Cysteine proteinases and inhibitors in inflammation: their role in periodontal disease. *J. Periodontol.* 1993, *64*, 485–491.

[22] Surna, A., Kubilius, R., Sakalauskiene, J., Vitkauskiene, A. et al., Lysozyme and microbiota in relation to gingivitis and periodontitis. *Med. Sci. Monit.* 2009, *15*, 66–73.

[23] Sorsa, T., Tjäderhane, L., Konttinen, Y. T., Lauhio, A. et al., Matrix metalloproteinases: contribution to pathogenesis, diagnosis and treatment of periodontal inflammation. *Ann. Med.* 2006, *38*, 306–321.

[24] Nonnenmacher, C., Helms, K., Bacher, M., Nüsing, R. M. et al., Effect of age on gingival crevicular fluid concentrations of MIF and PGE2. *J. Dent. Res.* 2009, *88*, 639–643.

[25] Krayer, J. W., Emerson, D. L., Goldschmidt-Clermont, P. J., Nel, A. E. et al., Qualitative and quantitative studies of Gc (vitamin D-binding protein) in normal subjects and patients with periodontal disease. *J. Periodontal Res.* 1987, *22*, 259–263.

[26] Verstappen, J., Von den Hoff, J. W., Tissue inhibitors of metalloproteinases (TIMPs): their biological functions and involvement in oral disease. *J. Dent. Res.* 2006, *85*, 1074–1084.

[27] Kontush, A., Chapman, M. J., Antiatherogenic small, dense HDL–guardian angel of the arterial wall? *Nat. Clin. Pract. Cardiovasc. Med.* 2006, *3*, 144–153.

[28] Zelko, I. N., Mariani, T. J., Folz, R. J., Superoxide dismutase multigene family: a comparison of the CuZn-SOD (SOD1), Mn-SOD (SOD2), and EC-SOD (SOD3) gene structures, evolution, and expression. *Free Radic. Biol. Med.* 2002, *33*, 337–349.

[29] Schittek, B., Hipfel, R., Sauer, B., Bauer, J. et al., Dermcidin: a novel human antibiotic peptide secreted by sweat glands. *Nat. Immunol.* 2001, *12*, 1133–1137.

[30] Hartroth, B., Seyfahrt, I., Conrads, G., Sampling of periodontal pathogens by paper points: evaluation of basic parameters. *Oral. Microbiol. Immunol.* 1999, *14*,326–330.

[31] Kardeşler, L., Buduneli, N., Biyikoğlu, B., Cetinkalp, S. et al., Gingival crevicular fluid PGE2, IL-1beta, t-PA, PAI-2 levels in type 2 diabetes and relationship with periodontal disease. *Clin. Biochem.* 2008, *41*, 863–868.

[32] Leitch, J. M., Yick, P. J., Culotta, V. C., The right to choose: multiple pathways for activating copper, zinc superoxide dismutase. *J. Biol.Chem.* 2009, *284*, 24679–24683.

[33] Zhang, C., Walker, L. M., Hinson, J. A., Mayeux, P. R., Oxidant stress in rat liver after lipopolysaccharide administration: effect of inducible nitric-oxide synthase inhibition. *J. Pharmacol. Exp. Ther.* 2000, *293*, 968–972.

[34] Zhang, C., Walker, L. M., Mayeux, P. R., Role of nitric oxide in lipopolysaccharide-induced oxidant stress in the rat kidney. *Biochem. Pharmacol.* 2000, *59*, 203–209.

[35] Kimura, S., Yonemura, T., Kaya, H., Increased oxidative product formation by peripheral blood polymorphonuclear leukocytes in human periodontal diseases. *J. Periodontal. Res.* 1993, *28*, 197–203.

[36] Akalin, F. A., Toklu, E., Renda, N., Analysis of superoxide dismutase activity levels in gingiva and gingival crevicular fluid in patients with chronic periodontitis and periodontally healthy controls. *J. Clin. Periodontol.* 2005, *32*, 238–243.

[37] O'Brien-Simpson, N. M., Pathirana, R. D., Paolini, R. A., Chen, Y. Y. et al., An immune response directed to proteinase and adhesin functional epitopes protects against Porphyromonas gingivalis-induced periodontal bone loss. *J. Immunol.* 2005, *175*, 3980–3989.

[38] Hajishengallis, G., Porphyromonas gingivalis-host interactions: open war or intelligent guerilla tactics? *Microbes. Infect.* 2009, *11*, 637–645.

[39] Socransky, S. S., Haffajee, A. D., Dental biofilms: difficult therapeutic targets. *Periodontol 2000.* 2002, *28*, 12–55.

[40] Teles, R. P., Gursky, L. C., Faveri, M., Rosa, E. A. et al., Relationships between subgingival microbiota and GCF biomarkers in generalized aggressive periodontitis. *J. Clin. Periodontol.* 2010, *37*, 313–323.

Hindawi Publishing Corporation
International Journal of Proteomics
Volume 2012, Article ID 108609, 8 pages
doi:10.1155/2012/108609

Research Article

Identification of a Novel Biomarker for Biliary Tract Cancer Using Matrix-Assisted Laser Desorption/Ionization Time-of-Flight Mass Spectrometry

Shintaro Kikkawa,[1] Kazuyuki Sogawa,[2] Mamoru Satoh,[2] Hiroshi Umemura,[3] Yoshio Kodera,[2,4] Kazuyuki Matsushita,[3] Takeshi Tomonaga,[2,5] Masaru Miyazaki,[6] Osamu Yokosuka,[1] and Fumio Nomura[2,3]

[1] *Department of Medicine and Clinical Oncology, Graduate School of Medicine, Chiba University, 1-8-1 Inohana, Chuo-ku, Chiba, Chiba City 260-8670, Japan*
[2] *Clinical Proteomics Center, Chiba University Hospital, 1-8-1 Inohana, Chuo-ku, Chiba, Chiba City 260-8670, Japan*
[3] *Department of Molecular Diagnosis, Graduate School of Medicine, Chiba University, 1-8-1 Inohana, Chuo-ku, Chiba, Chiba City 260-8670, Japan*
[4] *Department of Physics, School of Science, Kitasato University, 1-15-1 Kitasato, Minami-ku, Kanagawa, Sagamihara City 228-8555, Japan*
[5] *Laboratory of Proteome Research, National Institute of Biomedical Innovation, 7-6-8 Saito Asagi, Osaka, Ibaraki City 567-0085, Japan*
[6] *Department of General Surgery, Graduate School of Medicine, Chiba University, 1-8-1 Inohana, Chuo-ku, Chiba, Chiba City 260-8670, Japan*

Correspondence should be addressed to Fumio Nomura, fnomura@faculty.chiba-u.jp

Received 10 January 2012; Accepted 9 June 2012

Academic Editor: Terence C. W. Poon

Early diagnosis of biliary tract cancer (BTC) is important for curative surgical resection. Current tumor markers of BTC are unsatisfactory in terms of sensitivity and specificity. In a search for novel biomarkers for BTC, serum samples obtained from 62 patients with BTC were compared with those from patients with benign biliary diseases and from healthy controls, using the MALDI-TOF/TOF ClinProt system. Initial screening and further validation identified a peak at 4204 Da with significantly greater intensity in the BTC samples. The 4204 Da peak was partially purified and identified as a fragment of prothrombin by amino acid sequencing. The sensitivity of the 4204 Da peptide for detection of stage I BTC cancer was greater than those for CEA and CA19-9. Also, serum levels of the 4204 Da peptide were above the cut-off level in 15 (79%) of 19 cases in which the CEA and CA19-9 levels were both within their cut-off values. Receiver operating characteristic analysis showed that the combination of the 4204 Da peptide and CA19-9 was significantly more sensitive for detection of stage I BTC cancer compared to CEA and CA19-9. These results suggest that this protein fragment may be a promising biomarker for biliary tract cancer.

1. Introduction

Biliary tract cancer (BTC) is a neoplasm that accounts for 3% of all gastrointestinal cancers and 15% of all primary liver cancers. Over the last two decades, the incidence of BTC has risen, mainly due to an increase in the intrahepatic form [1, 2], which has a particularly high incidence in Northern Thailand [3]. Surgical resection is the only curative treatment and this requires an early diagnosis. Even in cases in which surgical resection with negative histological margins is achieved, the 5-year survival rates range from 20% to 40% [4, 5]. The mean one-year survival rate for unresectable cases is only 6 months [4]. Therefore, there is a need to establish a tool for early diagnosis of BTC. Currently, diagnosis of

Table 1: Clinical characteristics of patients with biliary tract cancer or benign biliary disease and healthy volunteers.

Healthy volunteers	Benign biliary disease	Biliary tract cancer	
No. of patients	30	30	62
Male/female	18/12	18/12	36/26
Mean age	65.5 ± 4.5	64.4 ± 39.0	64.7 ± 37.4
CEA (ng/mL)	3.1 ± 3.5	2.5 ± 3.6	37.6 ± 1577.3
CA19-9 (U/mL)	15.3 ± 18.6	70.4 ± 603.9	5033.6 ± 190367.2

BTC depends on imaging of the biliary tree using computed tomography (CT), ultrasonography, and endoscopic retrograde cholangiography (ERC) in symptomatic subjects. Brush cytology during ERC can lead to morphological diagnosis, but the sensitivity is limited because of the highly desmoplastic reaction of BTC [5, 6]. For these reasons, tumor markers that can detect BTC with high diagnostic efficiency are urgently needed. Carcinoembryonic antigen (CEA) and carbohydrate antigen 19.9 (CA19-9) are tumor markers that are used for diagnosis of BTC, but their sensitivity and specificity are unsatisfactory [2, 7].

Proteome analysis is increasingly being applied to cancer biomarker discovery. Surface enhanced laser desorption/ionization time-of-flight mass spectrometry (SELDI-TOF MS) is a proteomics technique used for high-throughput fingerprinting of serum proteins [8]. We have used this technology to identify diagnostic markers for alcohol abuse [9] and a prognostic marker for pancreatic cancer [10]. SELDI-TOF MS can be used to analyze many samples rapidly and simultaneously, but has drawbacks of high cost and difficulty with protein identification. More recently, high-throughput workflow with matrix-assisted laser desorption/ionization-time of flight/time of flight-mass spectrometry (MALDI-TOF/TOF MS) has been established for discovery and identification of serum peptides [11]. This method uses magnetic beads with different chemical chromatographic surfaces, instead of ProteinChip arrays. Proteins selectively bound to the magnetic beads are eluted and analyzed by MALDI-TOF/TOF MS. Compared with the SELDI-TOF MS ProteinChip system, the cost is low, and subsequent protein identification is relatively easy. We recently used the ClinProt system for MALDI-TOF/TOF MS to detect novel biomarkers for alcohol abuse that could not be detected using SELDI [12]. In the present study, we carried out a serum peptidome study to identify novel biomarkers for biliary tract cancer using the MALDI-TOF/TOF MS ClinProt system.

2. Methods

2.1. Patients and Samples. Serum samples were obtained from 62 patients with BTC (36 males, 26 females; median age 64.7 years old, range 27–81 years old), 30 age-matched healthy controls (18 males, 12 females; median age 65.5 years old, range 61–69 years old), and 30 age-matched patients with benign biliary disease (18 males, 12 females; median age 64.4 years old, range 27–90 years old). Clinicopathological data for all the subjects are shown in Tables 1, 2, and 3. The

Table 2: Characteristics of patients with biliary tract cancer.

Item	Number of patients
Location	
Extrahepatic	16
Intrahepatic	17
Klatskin	7
Ampulla of Vater	6
Gallbladder	16
UICC stage	
Stage I	6
Stage II	10
Stage III	16
Stage IV	30

Table 3: Characteristics of patients with benign biliary disease (n = 30).

Item	Number of patients
Cholelithiasis	26
Benign fibrous stricture	2
Primary sclerosing cholangitis	2

BTC group (Table 2) included cases of intrahepatic cholangiocarcinoma (n = 17), Klatskin tumor (n = 7), extrahepatic cholangiocarcinoma (n = 16), tumor of the ampulla of Vater (n = 6), and gallbladder tumor (n = 16). The pathological stages of the BTC patients were defined according to the Union Internationale Contre le Cancer tumor node metastasis classification [13]. The patients with benign biliary diseases (Table 3) included cases of cholelithiasis (n = 24), benign fibrous stricture (n = 4), and primary sclerosing cholangitis (n = 2). All the cases of BTC were diagnosed by radiological imaging. In 58 cases, cytology was also compatible with the diagnosis. All of the patients with benign biliary disease were diagnosed by endoscopic retrograde cholangiopancreatography and were followed up for more than 12 months to confirm that they had no malignancy. Serum samples were obtained and processed under standardized conditions that we have described elsewhere [14] and were stored at −80°C until analysis. Written informed consent was obtained from all the subjects. The study was approved by the Ethics Committee of Chiba University School of Medicine.

2.2. Serum Pretreatment with Magnetic Beads Using the ClinProt Robot. We used weak cation exchange (WCX) magnetic

beads (Bruker Daltonics) and performed serum peptidome fractionation according to the manufacturer's protocol. A 5 μL serum sample was mixed with 10 μL of binding buffer to which 5 μL of WCX beads was added, and the solution was carefully mixed. The peptides in the serum were then allowed to bind to the WCX beads for 5 min. The tube was then placed in a magnetic bead separator (Bruker Daltonics) for separating unbound beads, and the supernatant was removed. The beads were washed three times with 100 μL of washing buffer, and the proteins as well as peptides were then eluted from the magnetic beads with 10 μL each of elution and stabilization buffer. Thereafter, 2 μL of peptide elution solution was mixed with 20 μL of alpha-cyano-4-hydroxy-cinnamic acid matrix (Bruker Daltonics). Then 0.8 μL of this mixture was spotted onto an AnchorChip target plate (Bruker Daltonics) and crystallized. Each sample was duplicated, and quadruplicate spotting was performed using each eluate; eight spots were developed from each sample. The mean spectra from these eight spots were used for data analyses. These procedures from bead fractionation to spotting were performed automatically using the ClinProt robot (Bruker Daltonics) under strictly controlled humidity, as we previously described [14].

2.3. Mass Spectrometry. The AnchorChip target plate was placed in an AutoFlex II TOF/TOF mass spectrometer (Bruker Daltonics) controlled by Flexcontrol 2.4 software (Bruker Daltonics). The instrument was equipped with a 337 nm nitrogen laser, delayed-extraction electronics, and a 25 Hz digitizer. All acquisitions were generated by an automated method included in the instrument software and based on averaging of 1000 randomized shots. Spectra were acquired in positive linear mode in the mass range of 600–10000 Da. Peak clusters were completed using second pass peak sections (signal to noise ratio > 5). The relative peak intensities of *m/z* between 600 and 10000 normalized to a total ion current were expressed in arbitrary units. Calibration was performed using Peptide Calibration Standard II (Bruker Daltonics). All MALDI-TOF MS spectra from *m/z* 1000 to 10000 were analyzed with FlexAnalysis 2.1 and ClinProtools 2.1 software (Bruker Daltonics).

2.4. Protein Identification. A CM ceramic Hyper DF spin column (Bio-Rad Laboratories, Irvine, CA, USA) was washed 3 times with 400 μL of MB-WCX binding solution (Bruker Daltonics). Serum samples (320 μL) were diluted 5-fold with binding buffer and the diluted sample (1600 μL) was applied to the spin column. The sample was allowed to bind at 4°C for 1 h on a shaker and then the spin column was washed 3 times with 400 μL of binding buffer. Finally, 320 μL of MB-WCX stabilization solution (Bruker Daltonics) was added to the spin column for elution. Ten volumes of ice cold acetone were added to the eluate. Peptides/proteins were allowed to precipitate at −20°C for 2 h and then obtained by centrifugation at 13000 g for 10 min at 4°C. After decanting the acetone, the peptides/proteins were allowed to air dry. The dried pellets were resuspended in buffer (0.1% trifluoroacetic acid in water, vol/vol) and further separated by reversed-phase HPLC in an automated HPLC system (Shiseido Nanospace SI-2, Shiseido Fine Chemicals, Tokyo, Japan). The concentrated flow-through sample (75 μL) was directly loaded onto an Intrada WP-RP column (Imtakt, Kyoto, Japan). The reversed-phase separations for each flow-through fraction were performed using a multisegment elu-k tion gradient with eluent A (0.1% trifluoroacetic acid in water, vol/vol) and eluent B (0.08% trifluoroacetic acid in 90% acetonitrile, vol/vol). The gradient elution program consisted of three steps with increasing concentrations of eluent B (5% B for 5 min, 5% to 95% B for 23 min, and 95% B for 11 min) followed by 5% B for 21 min for reequilibration of the column at a flow rate of 0.40 mL/min for a total run time of 60 min. Based on the chromatogram recorded by measuring the absorbance of the eluate at 280 nm, fractions eluted at retention times between 19.1 and 39.1 min were collected in 40 0.2 mL aliquots at a fraction size setting of 0.5 min. Fractions including objective peaks were confirmed by MALDI-TOF MS. N-terminal amino acid sequence analysis was performed using a Procise 494 cLC protein sequencing system (Applied Biosystems, Foster City, CA, USA).

TABLE 4: Discriminatory peaks and *P* values in the training set.

Higher in biliary tract cancer group		Lower in biliary tract cancer group	
m/z	*P* value	*m/z*	*P* value
1207	<0.0001	1944	<0.0001
1466	<0.0001	2669	<0.001
3261	<0.001	2931	<0.0001
3950	<0.001	3239	<0.0001
4202	<0.001	3272	<0.001
4635	<0.001	3878	<0.01
4654	<0.001	4051	<0.001
5791	<0.0001	4086	<0.0001
5890	<0.0001	4276	<0.0001
5929	<0.001	6414	<0.001
9246	<0.001		
9285	<0.0001		

2.5. Statistical Analysis. Univariate analysis of individual peaks was performed using a nonparametric Mann-Whitney *U* test, with $P < 0.05$ considered significant. Discriminatory power for putative markers was further evaluated by receiver operating characteristic (ROC) analysis and the area under the curve (AUC) using IBM SPSS Statistics 18 (SPSS Inc., Ill, USA).

3. Results

3.1. MALDI-TOF-MS Analysis of Peptides in BTC Sera. As a first step, we compared the peptide profiles of serum samples obtained from BTC patients ($n = 30$) with those from healthy controls ($n = 12$) as a training set (Table 4). Totally 134 peaks were detected and compared in the MALDI

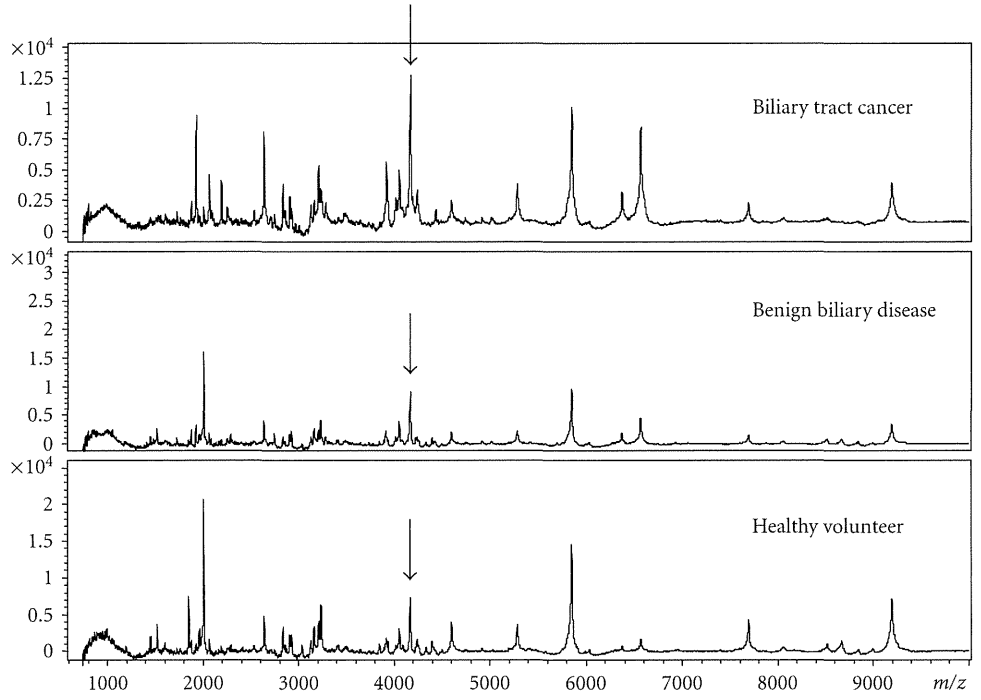

FIGURE 1: The protein mass profile between *m/z* 0 and 10000 highlighting the differentially expressed peaks in serum from healthy volunteers, patients with benign biliary disease, and BTC patients. The *m/z* 4204 peak (indicated by arrows) intensity was higher in cancer patients compared with patients with benign disease and healthy volunteers.

proteomic profile. Total of 22 peak intensities differed significantly between the BTC patients and healthy controls, including 12 that were higher and 10 that were lower in the BTC group. In typical spectra for serum samples from each group (Figure 1), the intensity of the 4204 *m/z* peak was higher in BTC samples compared with those from patients with benign biliary diseases and from healthy controls.

Next, we tested whether the differences observed in the 22 peaks in the training set were reproducible in another set of samples (test set) (Table 5). 32 BTC patients, 30 benign biliary patients, and 18 healthy controls were included in the test set. Out of these 22 peaks, the intensities of 2 peaks (3272 *m/z* and 4204 *m/z*) were again significantly different between the BTC and control groups. Out of these 2 peaks, the intensity of one peak (4204 *m/z*) was also found to be significantly higher in the BTC group compared to the benign disease group. The relative intensities of the 4204 *m/z* peak in sera obtained from the three groups of subjects are summarized in Figure 2.

3.2. Identification of the 4204 Da Peptide as a Fragment of Prothrombin. Partial purification of the peptide corresponding to the 4204 *m/z* peak was conducted as outlined in Section 2. N-terminal amino acid sequencing of trypsin digests of the final preparation containing the 4204 Da peptide revealed that it was a fragment of prothrombin (Figure 3).

3.3. Diagnostic Value of the 4204 Da Peptide Compared with Conventional Markers. Patients with BTC were divided into 4 groups based on clinical stage. The sensitivities of CEA, CA19-9, and 4204 Da in the BTC patients were determined (Figure 4). The optimal cut-off point for CEA, CA19-9, and the 4204 Da peptide were selected based on mean + 2SD in healthy subjects. The cut-off levels for CEA, CA19-9, and the 4204 Da peptide were set at 6.4 ng/mL, 33.5 U/mL, and 372.1 AU, respectively. The sensitivities of CEA, CA19-9, and the 4204 Da peptide in stage IV patients were 33.3%, 80.0%, and 66.7%, and the specificities of CEA, CA19-9, and the 4204 Da peptide were 93.3%, 93.3%, 96.7%, respectively. In contrast, these sensitivities in stage I patients were 0.0%, 16.7%, and 50.0%, and these specificities were 93.3%, 93.3%, 96.7%. The sensitivity of the 4204 Da peptide was also greater than those of CEA and CA19-9 in stage II patients.

The ROC curves for the 4204 Da peptide, CEA, and CA19-9 as single markers and combinations are shown in Figure 5. The sensitivities were determined from the results for the 62 patients with BTC and specificities were based on the 60 non-BTC subjects. The AUCs for the 4204 Da peptide, CEA, and CA19-9 as single markers were 0.75, 0.60, and 0.732, respectively. The AUC for the combination of the 4204 Da peptide and CA19-9 was significantly greater than

TABLE 5: Discriminatory peaks detected in the training set and test set.

Higher in biliary tract cancer group		Lower in biliary tract cancer group	
m/z	*P* value	*m/z*	*P* value
4202	<0.001	3272	<0.001

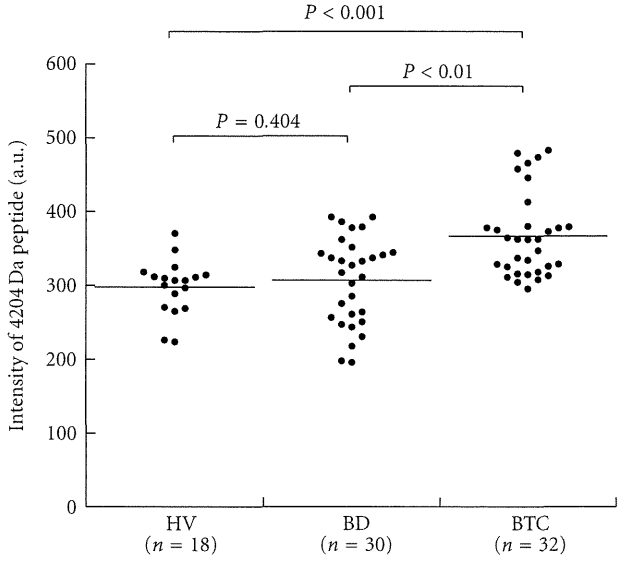

FIGURE 2: Normalized intensities of the peak corresponding to the 4204 Da peptide in serum from healthy volunteers (n = 18), patients with benign biliary disease (n = 30), and BTC patients (n = 32). The peak intensity was significantly higher in sera obtained from patients with biliary tract cancer (BTC) compared with sera from healthy volunteers. There was no significant difference in intensity between BTC sera and benign biliary disease (BB) sera (Mann-Whitney U test).

Prothrombin fragment detected in this study

MAHVRGLQLP GCLALAALCS LVHSQHVFLA PQQARSLLQR VRRANTFLEE VRKGNLEREC
VEETCSYEEA FEALESSTAT DVFWAKYTAC ETARTPRDKL AACLEGNCAE GLGTNYRGHV
NITRSGIECQ LWRSRYPHKP EINSTTHPGA DLQENFCRNP DSSTTGPWCY TTDPTVRRQE
CSIPVCGQDQ VTVAMTPRSE GSSVNLSPPL EQCVPDRGQQ YQGRLAVTTH GLPCLAWASA
QAKALSKHQD FNSAVQLVEN FCRNPDGDEE GVWCYVAGKP GDFGYCDLNY CEEAVEEETG
DGLDEDSDRA IEGRTATSEY QTFFNPRTFG SGEADCGLRP LFEKKSLEDK TERELLESYI
DGRIVEGSDA EIGMSPWQVM LFRKSPQELL CGASLISDRW VLTAAHCLLY PPWDKNFTEN
DLLVRIGKHS RTRYERNIEK ISMLEKIYIH PRYNWRENLD RDIALMKLKK PVAFSDYIHP
VCLPDRETAA SLLQAGYKGR VTGWGNLKET WTANVGKGQP SVLQVVNLPI VERPVCKDST
RIRITDNMFC AGYKPDEGKR GDACEGDSGG PFVMKSPFNN RWYQMGIVSW GEGCDRDGKY
GFYTHVFRLK KWIQKVIDQF GE

FIGURE 3: N-terminal amino acid sequence of the purified fraction. Red letters identify the N-terminal sequence. The molecular weight of the underlined region is 4204 Da.

that for CEA and CA19-9 (P < 0.01). The sensitivity and specificity for combination of the 4204 Da and CA19-9 were 59.8% and 84.0%.

The 62 patients with BTC were also classified into 8 groups based on their tumor marker status, as shown in Table 6. The cut-off values for CEA and CA19-9 were set at 5 ng/mL and 37 U/mL, respectively. The optimal cut-off point for the 4204 Da peptide was selected based on the ROC analysis. The 4204 Da peptide level was greater than the cut-off value in 15 (79%) of 19 cases in which the CEA and CA19-9 levels were within their respective cut-off values.

TABLE 6: Positive or negative status of 4204 Da peptide, CEA, and CA19-9 in patients with biliary tract cancer.

CEA (≥5 ng/mL)	CA19-9 (≥37 U/mL)	4204 Da peptide (≥322 A.U.)	Number of patients
−	−	−	4
−	−	+	15
−	+	−	6
+	−	−	2
+	+	−	3
+	−	+	2
−	+	+	18
+	+	+	12

4. Discussion

The sequencing of the human genome has opened the door for comprehensive analysis of all mRNAs (transcriptome) and proteins (proteome). However, the levels of mRNAs are not necessarily predictive of the corresponding protein levels. Indeed, a recent report indicated that the consistency between cDNA microarray and proteome-based profiles is limited for identification of candidate biomarkers in renal cell carcinoma [15]. Therefore, proteome analysis is a prerequisite for identification of novel biomarkers.